

PSFC/RR-83-17

**TWO DIMENSIONAL AND RELATIVISTIC EFFECTS
IN LOWER-HYBRID CURRENT DRIVE***

D. Hewett, K. Hizanidis, V. Krapchev and A. Bers

**Plasma Fusion Center
Massachusetts Institute of Technology
Cambridge, Massachusetts 02139**

Invited paper, for:

Proceedings of the IAEA Technical Committee Meeting on Non-Inductive Current Drive in Tokamaks, Culham, U.K., April 18-21, 1983.

TWO-DIMENSIONAL AND RELATIVISTIC EFFECTS IN LOWER-HYBRID CURRENT DRIVE*

D. Hewett, K. Hizanidis, V. Krapchev and A. Bers

Plasma Fusion Center
Massachusetts Institute of Technology
Cambridge, Massachusetts 02139

Abstract

We present new numerical and analytic solutions of the two-dimensional Fokker-Planck equation supplemented by a parallel quasilinear diffusion term. The results show a large enhancement of the perpendicular temperature of both the electrons resonant with the applied RF fields and the more energetic electrons in the tail. Both the RF generated current and power dissipated are substantially increased by the perpendicular energy broadening in the resonant region. In the presence of a small DC electric field the RF current generated is very much enhanced, much more than in a simple additive fashion. In addition we present a relativistic formulation of the two-dimensional Fokker-Planck quasilinear equation. From conservation equations, based upon this formulation, we derive the characteristics of RF current drive with energetic electrons. These show how the RF driven current and its figure of merit (I/P_d) increase with the energy of the current-carrying electrons, and that their perpendicular, random momentum must also increase.

The results are relevant to recent experiments of lower-hybrid current drive on Alcator C and PLT in which the applied RF spectra are resonant with very energetic electrons, and in which large perpendicular temperatures of the energetic electrons have been observed. It is pointed out that substantial improvements in the figure of merit, (I/P_d), of present experiments may be achieved by current drive with fast-waves in the lower-hybrid frequency range. The ultimate limitation in this type of current drive is likely to be the confinement of the very energetic electrons.

* Work supported by DOE Contract No. DE-AC02-78ET-51013.

Duplicate

I. INTRODUCTION

The past year has witnessed major progress in lower-hybrid current drive experiments on large tokamak plasmas [1,2]. These have demonstrated the maintenance of considerable currents by the RF in the absence of the ohmic (DC) electric field. An important feature of these experiments is that the excited RF spectra have phase velocities that are resonant with very energetic electrons, fifty to a few hundred times the thermal energy of the bulk plasma which was about 1 keV in both experiments. Both experiments show that the RF generated current is carried by electrons effectively in the 50-100 keV range and is characterized by a perpendicular temperature which is of the same order in energy [3,4].

An analysis of RF current drive based upon the Fokker-Planck equation for treating collisions and quasilinear diffusion was first given by Klima and Sizonenko [5]; they, however, did not recognize that substantial current can be carried by a plateau of resonant electrons when the RF power is sufficiently high. Later, in a one-dimensional Fokker-Planck theory it was pointed out that such a plateau exists and it may be maintained by an acceptably small power density [6]. A numerical two-dimensional Fokker-Planck study [7] came to the conclusions that the "figure of merit" – current density divided by power dissipated – is increased by a factor of nearly 2, compared to [6] but no change in the current itself was found. Neither the current generated nor the large perpendicular temperature can be understood or predicted from any of the available theoretical or numerical works. Finally, none of the previous theoretical or numerical analyses have addressed in full the relativistic effects in current drive with energetic electrons.

In this paper we present our recent theoretical and numerical results relevant to an understanding of these current drive experiments. In section II we present a new numerical integration of the two-dimensional Fokker-Planck equation supplemented by a DC electric field term and a quasilinear diffusion term due to the RF. These results exhibit the large perpendicular temperature enhancement in the resonant electrons and the more energetic electrons in the tail. The results also show how this effect varies with the position and width of the applied RF spectrum. An analytical description of these results, based upon an approximate solution of the

two-dimensional Fokker-Planck plus quasilinear equation, is given in section III. Here we show that the large enhancement in the perpendicular temperature increases both the current generated and the power dissipated, and thus their ratio remains essentially unchanged. Finally, in section IV we give a relativistic formulation of the two-dimensional Fokker-Planck equation and quasilinear diffusion appropriate for lower-hybrid current drive. The conservation equations that follow from the moments of this equation are used to derive the properties of the steady-state RF current drive for an effective distribution function in two-dimensional momentum space. A relativistic limit to the figure of merit is derived, and improvement in the currently achieved figure of merit is suggested through the use of fast waves in the lower-hybrid range of frequencies for driving current with more energetic electrons. The derived steady state also shows that with larger parallel momenta there must be a larger perpendicular, random momentum. Thus lower-hybrid current drive with energetic electrons will probably be limited by how well such electrons can be confined in the plasma.

II. NUMERICAL SOLUTIONS

One method of investigation of the two-dimensional effects of lower-hybrid-current drive is to solve numerically the relevant Fokker-Planck equation supplemented with an appropriate quasilinear diffusion term. The complete nonlinear Fokker-Planck equation is a rather ambitious and expensive numerical task. We have chosen an approximation for the Fokker-Planck operator – one more appropriate to our needs. Following Karney and Fisch [7], we use an operator that is linearized because we expect that, even with the largest amplitudes for the drive fields, the bulk distribution will remain nearly Maxwellian. We also ignore all spatial gradients – preferring to avoid the complexity and computational expense in order to understand more completely the behavior of the electron distribution in velocity space under the influence of the RF diffusion.

The problem we solve numerically here is a linearized Fokker-Planck operator, valid for $v/v_{thermal} \gg 1$, due to Gurevich and Lebedev [8], in which we have added an additional term due to parallel, quasilinear RF diffusion. The form of the equation is

$$\frac{\partial f}{\partial \tau} + E_0 \frac{\partial f}{\partial v_{\parallel}} - \frac{\partial}{\partial v_{\parallel}} \left[D(v_{\parallel}) \frac{\partial f}{\partial v_{\parallel}} \right] - \frac{1}{u^2} \frac{\partial}{\partial u} \left[\frac{1}{u} \frac{\partial f}{\partial u} + f \right] - \frac{1}{u^3} \frac{\partial}{\partial \mu} \left[(1 - \mu^2) \frac{\partial f}{\partial \mu} \right] = 0 \quad (1)$$

where

$$\frac{\partial}{\partial v_{\parallel}} = \mu \frac{\partial}{\partial u} + \frac{(1 - \mu^2)}{u} \frac{\partial}{\partial \mu} \quad (2)$$

and $u^2 = v_{\parallel}^2 + v_{\perp}^2$, $\mu = v_{\parallel}/u = \cos \theta$; u is the velocity magnitude in spherical coordinates and θ is the polar angle with respect to the DC electric and magnetic fields, both of which are in the same direction (\parallel). Symmetry is assumed in the azimuthal coordinate. We work with the coordinates (u, μ) rather than $(v_{\parallel}, v_{\perp})$ but we use the v_{\parallel} representation to make the physics more transparent. The time variable τ is scaled by the Coulomb collision time and u is normalized to $v_{thermal}$. E_0 is an externally applied DC electric field and D is a RF diffusion amplitude resulting from the application of external microwave power. Since the coupling of RF power from the antenna to the inhomogeneous plasmas of interest here are not yet well understood, we choose a model form

$$D(v_{\parallel}) = D_0 \exp \left[- \frac{(v_{\parallel} - v_0)^p}{(\Delta v)^p} \right] \quad (3)$$

for the diffusion coefficient, which implies that the RF power spectrum inside the plasma is

$$|E_{\parallel}(\omega, k)|^2 \simeq \frac{1}{k} \quad (4)$$

where k is the wavenumber parallel to the DC magnetic field. We find it numerically advantageous to split the distribution function

$$f(u, \mu) = f_0(u) + f_1(u, \mu) \quad (5)$$

$$f_0(u) = \exp(-u^2/2) \quad (6)$$

although there is no requirement that f_1 be small. We can expect the solution of Eq. (1) to be useful only for electric fields E_0 sufficiently small that the critical velocity $v_c \simeq E_0^{-1/2}$ is well above velocities of interest.

We solve Eq. (1) in the computational region displayed in Fig. 1. The annular region between $-1 \leq \mu \leq 1$ and $u_{min} \leq u \leq u_{max}$ is filled with a uniformly spaced mesh—typically with 80 points in u and 60 points in μ . The boundaries at $\mu = \pm 1$ are lines of symmetry. On these lines

$$\frac{\partial f}{\partial \mu} = \frac{\partial f_1}{\partial \mu} = 0 \quad (7)$$

Within the bulk of the plasma ($u \leq u_{min}$), Coulomb collisions are assumed sufficiently frequent to insure that there will never be any appreciable non-Maxwellian contribution. This condition is that $f_1(u_{min}, \mu) = 0$. The boundary at $u = u_{max}$ is expected to be sufficiently far out in magnitude so that $f(u_{max}, \mu)$ is negligible; physically, u_{max} is chosen large enough so that there are never appreciable particles to affect the distribution at smaller u .

The flux of particles through the boundaries at $\mu = \pm 1$ is obviously zero. The flux of particles through the other boundaries at u_{min} and u_{max} , given by

$$S_u = -\frac{1}{u^2} \left[\frac{1}{u} \frac{\partial f}{\partial u} + f \right] \quad (8)$$

is not zero; f_0 gives no contribution to S_u but a finite contribution is obtained from f_1 which may have arbitrary normal derivative on the two boundaries in question. Since we will be interested in the time asymptotic state, we note that the final state will be one that may exhibit arbitrary flow through the computational volume so long as all features within the region are time independent. Details of the computational techniques used are given in the Appendix.

In the initial applications, we considered several cases with finite RF diffusion and no DC electric field. In Fig. 2a we show a contour plot of the total distribution function f in which the contours are logarithmically placed starting with 1×10^{-8} on the outside. We have plotted levels 1, 4, and 7 within each decade. The innermost contour is 0.7. In this particular case, we have used $D_0 = 1$, $v_0 = 4$, $\Delta v = 1$, and $p = 4$. The distribution function is obviously elongated in the region in which the RF spectrum is applied. Several measures may be applied to the steady-state distributions: the first $v_{||}$ moment of the distribution is the parallel current J produced by this application of RF power. The dependence of J on the parameters

in $D(v_{\parallel})$ will be presented in section III. In Fig 2b we display the perpendicular temperature T_{\perp} given by

$$T_{\perp}(v_{\parallel}) = \int_0^{\infty} \frac{1}{2} v_{\perp}^3 f(v_{\parallel}, v_{\perp}) dv_{\perp} \quad (9)$$

as a function of v_{\parallel} . Particularly intriguing is the enhancement of the perpendicular temperature not only in the region in which the RF spectrum is applied but also in the region of v_{\parallel} well above the spectrum. The temperature apparently rises until there is no longer sufficient grid resolution to accurately perform the integration. The temperature enhancement in the RF region is suggested by an analytic solution presented in section III, but the large T_{\perp} for larger v_{\parallel} is not yet well understood. Fig. 3a and 3b are a similar set of plots for $D_0 = 1$, $v_0 = 6$, $\Delta v = 2$, and a reduced power in the exponent $p = 2$. This is a much broader spectrum centered at a larger v_0 . For this set of parameters the distribution function is stretched, understandably, farther in the positive v_{\parallel} direction. The enhancement of T_{\perp} is much larger in the RF spectrum range than for the first case shown in Fig. 2 and T_{\perp} becomes even larger above the RF range. Lack of resolution is a more severe problem in this case because the spectrum extends farther out in u . To properly resolve this case, we have nearly doubled the grid points in u ; this solution was obtained on a 150×60 mesh. With the increased resolution, the behavior of $T_{\perp}(v_{\parallel})$ for large v_{\parallel} can be more accurately displayed. Apparently, $T_{\perp}(v_{\parallel})$ does approach the asymptotic value of 1 for very large v_{\parallel} .

The numerical results presented here clearly point out the large enhancement of the perpendicular temperature associated with the current carrying electrons within the RF spectrum, and those in the tail beyond the RF spectrum, for lower-hybrid current drive. These features are borne out by recent experiments on lower-hybrid current drive on PLT [3] and Alcator C [4]. The increase of T_{\perp} in the resonant domain was pointed out in [7], but its consequences were not fully explored. As we point out in the next section, this introduces important modifications to both the current generated and power dissipated in lower-hybrid current drive.

Finally, applications of this numerical procedure with a finite DC electric field E_0 are at this writing just beginning. Our immediate purpose is to consider the

interaction of the RF current producing spectrum with a finite but small electric field – a field sufficiently small such that the runaway velocity $v_c \sim 1/\sqrt{E_0}$ is greater than u_{max} . Preliminary results indicate that the current that results from the interaction of RF power and E_0 are not additive. For example, with $E_0 = 0$, $D_0 = 0.2$, $v_0 = 4$, $p = 4$, and $\Delta v = 1$ we obtain a normalized current of 0.044; with $D_0 = 0$, and $E = 0.01$, the normalized current is 0.023. If these two current producing effects are simultaneously applied, the resulting current is 0.0872 – a value 30% higher than the algebraic sum of the individual effects.

III. THE STEADY STATE SOLUTION OF A TWO-DIMENSIONAL FOKKER-PLANCK EQUATION WITH STRONG RF DIFFUSION

The conclusions of previous numerical studies [7] were not based on an analytical solution, and the range of parameters studied was very limited. As shown in section II, we find numerically that for realistic spectra there is a substantial broadening of the distribution function in the perpendicular direction. This leads to a large T_\perp in the resonant domain of velocity space, compared with the bulk electron temperature T_B . As a result many more particles are carrying the current, since the number of particles in the plateau scales as T_\perp/T_B .

As an intermediate step we use for f the result of the 1D theory $f \sim \exp\left(\frac{1}{Dv_\parallel}\right)$, but with T_\perp different from T_B . Consider a model distribution function for the resonant plateau:

$$f = \exp\left(-\frac{v_\perp^2}{2T_\perp} + \frac{1}{Dv_\parallel}\right) \frac{\exp(-v_\parallel^2/2)}{\sqrt{2\pi}} \quad (10)$$

where velocities, temperature and diffusion coefficient are normalized to the bulk quantities. One can readily evaluate the current from

$$J = \int_0^\infty v_\perp dv_\perp \int_{v_1}^{v_2} v_\parallel dv_\parallel f \quad (11)$$

For $D \gg 1$ we find

$$J = \frac{e^{-v_1^2/2}}{\sqrt{2\pi}} T_\perp \frac{v_2^2 - v_1^2}{2} \quad (12)$$

But this is exactly the well known one-dimensional current multiplied by T_{\perp} . Similarly one can write for the power dissipated:

$$p_D = \int_0^{\infty} v_{\perp} dv_{\perp} \int_{v_1}^{v_2} \frac{v_{\parallel}^2 + v_{\perp}^2}{2} dv_{\parallel} D \frac{\partial^2 f}{\partial v_{\parallel}^2} \quad (13a)$$

An integration by parts gives

$$p_D = - \int_0^{\infty} v_{\perp} dv_{\perp} \int_{v_1}^{v_2} v_{\parallel} dv_{\parallel} D \frac{\partial f}{\partial v_{\parallel}} \quad (13b)$$

and the final result is:

$$p_D = \frac{e^{-v_1^2/2}}{\sqrt{2\pi}} T_{\perp} \ln \frac{v_2}{v_1} \quad (14)$$

Again, the power dissipated is enhanced by T_{\perp} compared with 1D theory; however, the ratio J/p_D is unchanged. This is not surprising, since J/p_D is a very insensitive quantity and does not represent a good check on either theory or computations. Obviously it is very important from a practical point of view, however, if J itself is wrongly estimated the whole energy balance will be misleading.

While the model distribution function (10) describes qualitatively the effect of the broadening in the perpendicular direction it does not satisfy the 2D Fokker-Planck equation. Now we proceed to solve for the steady state 2D distribution function in the resonant domain when $D \gg 1$. If we assume $D = \text{const.}$ for $v_1 \leq v \leq v_2$ the solution is of the form:

$$f = \varphi(v_{\perp}^2) \exp\left[\frac{1}{D} \psi(v_{\parallel}, v_{\perp})\right] \quad (15)$$

We substitute (15) in the steady state 2D Fokker-Planck equation and to order D^0 we obtain:

$$\frac{\partial^2 \psi}{\partial v_{\parallel}^2} \varphi + \frac{4v_{\parallel}^2}{(v_{\parallel}^2 + x)^{3/2}} (\varphi' + x\varphi'') = 0 \quad (16)$$

where $x \equiv v_{\perp}^2$ and $\varphi' = \frac{d\varphi}{dx}$. Eq. (16) is solved by separating the variables.

$$\frac{\partial^2 \psi}{\partial v_{\parallel}^2} = \frac{4v_{\parallel}^2}{(v_{\parallel}^2 + x)^{3/2}} \eta_0(x) \quad (17)$$

$$\eta_0 \varphi + \varphi' + x\varphi'' = 0. \quad (18)$$

Here η_0 is an arbitrary function of x to be determined from the boundary conditions. An integration of Eq. (17) over v_{\parallel} gives:

$$\frac{\partial \psi}{\partial v_{\parallel}} = \eta_1(x) + 4\eta_0(x) \left[\ln(v_{\parallel} + \sqrt{v_{\parallel}^2 + x}) - \frac{v_{\parallel}}{\sqrt{v_{\parallel}^2 + x}} \right] \quad (19)$$

$\eta_1(x)$ is also a function of x to be found from the boundary conditions.

We require that the distribution function and the parallel flux S_{\parallel} are continuous at $v_{\parallel} = v_1, v_2$. However, $\frac{\partial f}{\partial v_{\parallel}}(v_{\parallel} = v_1, v_2)$ will be discontinuous. We assume that for $v_{\parallel} \rightarrow v_1(v_{\parallel} < v_1)$ and $v_{\parallel} \rightarrow v_2(v_{\parallel} > v_2)$, $\frac{\partial f}{\partial v_{\parallel}} = -v_{\parallel} f$. This implies that outside the resonant domain the distribution function retains its Maxwellian character in the parallel direction. One should point out that this assumption is verified by the numerical integration. The expression for the parallel flux is:

$$S_{\parallel} = -\frac{v_{\parallel}}{v^3} \left(\frac{2x \frac{\partial}{\partial x} + v_{\parallel} \frac{\partial}{\partial v_{\parallel}}}{v^2} + 1 \right) f + \frac{1}{v^3} \left(2v_{\parallel} x \frac{\partial}{\partial x} - x \frac{\partial}{\partial v_{\parallel}} \right) f - D \frac{\partial f}{\partial v_{\parallel}} \quad (20)$$

where $v^2 = v_{\parallel}^2 + x$. For $v^2, D \gg 1$ we find to order D^0 with f given by (15):

$$S_{\parallel} = -\frac{v_{\parallel}}{v^3} (\varphi - 2x\varphi') - \varphi \frac{\partial \psi}{\partial v_{\parallel}} \quad (21)$$

The S_{\parallel} outside the resonance plateau ($D = 0$) is given by:

$$S_{\parallel} = -\frac{v_{\parallel}}{v^3} (\varphi - 2x\varphi') + \frac{v_{\parallel}}{v^3} \left(\frac{v_{\parallel}^2}{v^2} + x \right) \varphi \quad (22)$$

To write (22) we assume that $f \simeq \varphi$ and $\frac{\partial f}{\partial v_{\parallel}} \simeq -v_{\parallel} \varphi$ for $v \simeq v_1, v_2$. Thus we have incorporated the condition of continuity of the distribution function at the boundary and the assumption of a Maxwellian derivative in the parallel direction.

From (21) and (22) we obtain:

$$\frac{\partial \psi}{\partial v_{\parallel}} = -\frac{v_{\parallel}}{v^3} \left(\frac{v_{\parallel}^2}{v^2} + x \right) \quad \text{for } v_{\parallel} = v_1, v_2 \quad (23)$$

With the expression of $\frac{\partial \psi}{\partial v_{\parallel}}$ from Eq. (19) we determine $\eta_0(x)$ and $\eta_1(x)$. The result for $\eta_0(x)$ is substituted in Eq.(18) and we are left with a linear second order differential equation to solve. The numerical integration will be reported elsewhere. Here we would like to point out that for $x < v_1^2$, $\eta_0(x)$ takes the particularly simple form.

$$\eta_0(x) = (1+x)\alpha, \quad \alpha \equiv \frac{1}{4 \ln \frac{v_2}{v_1}} \frac{v_2^2 - v_1^2}{v_1^2 v_2^2} \quad (24)$$

From Eq. (18) it is easy to verify by direct substitution that approximately

$$\varphi \simeq \exp(-\alpha x - \frac{\alpha}{4} x^2). \quad (25)$$

Eq. (25) together with the expressions for η_0 , η_1 , from (19) and (23) determine completely the distribution function in the resonant domain. Note that the assumption of the 1D theory [6] was $\varphi = \exp(-\frac{x}{2})$. It fails to exhibit the important scaling of α with the position and width of the spectrum.

The current becomes

$$J = \frac{e^{-v_1^2/2}}{\sqrt{2\pi}} \cdot \frac{v_2^2 - v_1^2}{4} \int_0^{\infty} \varphi dx \quad (26)$$

With φ given by Eq. (25) we find

$$J = \frac{e^{-v_1^2/2}}{\sqrt{2\pi}} \cdot \frac{v_2^2 - v_1^2}{4} \sqrt{\frac{\pi}{\alpha}} e^{\alpha^2} [1 + \phi(\sqrt{\alpha})] \quad (27)$$

where ϕ is the error function. In all realistic spectra $\alpha \ll 1$ and (27) can be simplified.

$$J = \frac{e^{-v_1^2/2}}{\sqrt{2\pi}} \cdot \frac{v_2^2 - v_1^2}{4} \sqrt{\frac{\pi}{\alpha}}. \quad (28)$$

This formula is tested numerically and the results are compared with the 1D theory in Table I. It is clear that for a wide range of parameters the agreement with our theoretical result (28) is good, while the 1D theory predicts considerably less current. We calculate the power dissipated:

$$p_D = \frac{e^{-v_1^2/2}}{\sqrt{2\pi}} \int_0^\infty v_\perp dv_\perp \int_{v_1}^{v_2} dv_\parallel \frac{v_\parallel^2 + v_\perp^2}{2} \varphi \frac{\partial^2 \psi}{\partial v_\parallel^2} \quad (29)$$

From Eq. (16) we obtain

$$p_D = -\frac{e^{-v_1^2/2}}{\sqrt{2\pi}} \int_0^\infty dx \int_{v_1}^{v_2} dv_\parallel \frac{v_\parallel^2}{\sqrt{v_\parallel^2 + x}} (\varphi' + x\varphi'') \quad (30)$$

After an integration by parts we find:

$$p_D = \frac{e^{-v_1^2/2}}{2\sqrt{2\pi}} \int_0^\infty dx \int_{v_1}^{v_2} v_\parallel^2 dv_\parallel \varphi \frac{d}{dx} \left[\frac{x}{(v_\parallel^2 + x)^{3/2}} \right] \quad (31)$$

For $x < v_1^2$ the expression can be simplified to:

$$p_D = \frac{e^{-v_1^2/2}}{2\sqrt{2\pi}} \ln \frac{v_2}{v_1} \sqrt{\frac{\pi}{\alpha}} \quad (32)$$

Note that again the power dissipated is increased by $\alpha^{-1/2}$, which reflects the broadened distribution function.

Therefore the often cited ratio J/p_D remains unchanged:

$$J/p_D = \frac{v_2^2 - v_1^2}{2 \ln \frac{v_2}{v_1}} \quad (33)$$

The model distribution function (10) is justified by the correct 2D solution only in the sense that it shows the role a broadening in the perpendicular direction plays for determining J and p_D . Finally, we point out that recently attempts have been made to explain the discrepancy between the current estimated from 1D theory with a Brambilla-type calculation of the excited spectrum and the current observed in experiment by an upshift of the spectrum; the latter possibly due to toroidal

v_1	v_2	J_1	J_2	J_{num}
3	5	3.55×10^{-2}	1.68×10^{-1}	8.11×10^{-2}
3	6	5.98×10^{-2}	3.06×10^{-1}	1.87×10^{-1}
4	6	1.34×10^{-3}	8.11×10^{-3}	2.87×10^{-3}
3	7	8.87×10^{-2}	4.80×10^{-1}	3.34×10^{-1}
4	7	2.21×10^{-3}	1.43×10^{-2}	1.55×10^{-2}
5	7	1.78×10^{-5}	1.31×10^{-4}	5.59×10^{-5}
3	8	1.22×10^{-1}	6.92×10^{-1}	6.11×10^{-1}
4	8	3.21×10^{-3}	2.19×10^{-2}	1.98×10^{-2}
5	8	2.90×10^{-5}	2.26×10^{-4}	2.48×10^{-4}
6	8	8.51×10^{-8}	7.34×10^{-7}	7.77×10^{-7}

TABLE I

$v_1(v_2)$ are the low (high) velocity boundaries of the resonant region. From 1D theory $J_1 = \frac{e^{-v_1^2/2}}{\sqrt{2\pi}} \frac{v_2^2 - v_1^2}{2}$, and from 2D theory $J_2 = \frac{e^{-v_1^2/2}}{\sqrt{2}} \frac{v_1 v_2}{2} \sqrt{(v_2^2 - v_1^2) \ln \frac{v_2}{v_1}}$. J_{num} is the result of numerical integration.

effects, parametric processes, etc. With the present 2D results one needs much less of an upshift than previously thought.

IV. RELATIVISTIC THEORY FOR LOWER-HYBRID CURRENT DRIVE

As pointed out in section I, the recently successful and significant experiments on lower-hybrid current drive use RF spectra that are resonant with very energetic electrons. Hence, we now turn to an evaluation of such RF current drive based upon the relativistic Fokker-Planck equation with parallel diffusion due to the RF fields. Previous analysis of relativistic effects [9] was based upon a different model of current generation.

(a) The Relativistic Fokker-Planck Equation

For the collisional model we use the Lorentz limit of the relativistic Balescu-Lenard collision operator [10-11]. The collisional flux in momentum space is given by,

$$\begin{aligned} \tilde{S}_{\alpha\beta} = & -2q_\alpha^2 q_\beta^2 n_\beta \int d^3 p_\beta \int d^3 k \delta(\vec{k} \cdot \vec{v}_\alpha - \vec{k} \cdot \vec{v}_p) \frac{\vec{k} \vec{k} (1 - \vec{\beta}_\alpha \cdot \vec{\beta}_\beta)^2}{k^4 \left[1 - \left(\frac{\vec{k} \cdot \vec{\beta}_\alpha}{k} \right)^2 \right]^2} \\ & \cdot \left(\frac{\partial}{\partial \vec{p}_\alpha} - \frac{\partial}{\partial \vec{p}_\beta} \right) f_\alpha(\vec{p}_\alpha) f_\beta(\vec{p}_\beta) \end{aligned} \quad (34)$$

where the labels α and β refer to the test and the field species respectively, and the vector $\vec{\beta}$ is the relativistic beta: $\vec{\beta} = \frac{\vec{v}}{c} = \frac{\vec{p}}{mc\gamma}$ with m , γ , \vec{v} and \vec{p} being the rest mass, the relativistic gamma: $\gamma = (1 + p^2/m^2c^2)^{1/2}$, velocity and momentum, respectively. Furthermore q is the charge and n_β the density of the field species. It can be easily shown [12] that for non-relativistic field species the collisional flux $\tilde{S}_{\alpha\beta}$ reduces to,

$$\tilde{S}_{\alpha\beta} = - \int d^3 p_\beta \bar{\tau}_{\alpha\beta} \cdot \left(\frac{\partial}{\partial \vec{p}_\alpha} - \frac{\partial}{\partial \vec{p}_\beta} \right) f_\alpha(\vec{p}_\alpha) f_\beta(\vec{p}_\beta) \quad (35)$$

where the tensor $\bar{\tau}_{\alpha\beta}$ is defined as

$$\bar{\tau}_{\alpha\beta} = A_{\alpha\beta} \frac{|\vec{v}_\alpha - \vec{v}_\beta|^2 \bar{I} - (\vec{v}_\alpha - \vec{v}_\beta)(\vec{v}_\alpha - \vec{v}_\beta)}{|\vec{v}_\alpha - \vec{v}_\beta|^3} = A_{\alpha\beta} \frac{\partial^2}{\partial \vec{v}_\alpha \partial \vec{v}_\alpha} |\vec{v}_\alpha - \vec{v}_\beta| \quad (36)$$

with

$$A_{\alpha\beta} = 2\pi q_{\alpha}^2 q_{\beta}^2 n_{\beta} \ln \Lambda_{\alpha\beta}. \quad (37)$$

$\ln \Lambda_{\alpha\beta}$ is the Coulomb logarithm which corresponds to a relativistic particle (α) colliding with a non-relativistic one (β). For fast electron-electron or fast electron-heavy ion interaction it is given in [13].

The collisional flux given by Eq.(35) can also be written in the following form,

$$\vec{S}_{\alpha\beta} = -\bar{D}_{\alpha\beta} \cdot \frac{\partial f_{\alpha}}{\partial \vec{p}_{\alpha}} + \vec{F}_{\alpha\beta} f_{\alpha} \quad (38)$$

where the collisional diffusion tensor $\bar{D}_{\alpha\beta}$ and frictional force vector $\vec{F}_{\alpha\beta}$ are defined by,

$$\bar{D}_{\alpha\beta} = \int d^3 p_{\beta} \bar{\tau}_{\alpha\beta}, \quad \vec{F}_{\alpha\beta} = - \int d^3 p_{\beta} f_{\beta} \vec{\nabla}_{\vec{p}_{\beta}} \cdot \bar{\tau}_{\alpha\beta} \quad (39)$$

with $\vec{\nabla}_{\vec{p}_{\alpha}}$ is the gradient operator $\frac{\partial}{\partial \vec{p}_{\alpha}}$. As long as one considers fast test particles interacting with a thermal background of field particles the magnitude of the relative velocity $\vec{v}_{\alpha} - \vec{v}_{\beta}$ can be expanded around $v_{\alpha} = |\vec{v}_{\alpha}|$:

$$|\vec{v}_{\alpha} - \vec{v}_{\beta}| \simeq v_{\alpha} - \vec{v}_{\beta} \cdot \frac{\partial v_{\alpha}}{\partial \vec{v}_{\alpha}} + \frac{1}{2} \vec{v}_{\beta} \vec{v}_{\beta} : \frac{\partial^2 v_{\alpha}}{\partial \vec{v}_{\alpha} \partial \vec{v}_{\alpha}} \quad (40)$$

where we dropped terms of order $(v_{\beta}/v_{\alpha})^3$ and higher. Introducing the notation $\langle \dots \rangle$ for averaging over the field particle distribution ($\langle \dots \rangle = \int \dots f_{\beta} d^3 p_{\beta}$) and assuming that the thermal background does not carry a current (i.e. $\langle \vec{v}_{\beta} \rangle = \vec{0}$) yields for the diffusion tensor,

$$\frac{\bar{D}_{\alpha\beta}}{A_{\alpha\beta}} = \frac{\bar{I} v_{\alpha}^2 - \vec{v}_{\alpha} \vec{v}_{\alpha}}{v_{\alpha}^3} - \frac{\langle v_{\beta}^2 \rangle}{v_{\alpha}^2} \frac{\bar{I} v_{\alpha}^2 - 3 \vec{v}_{\alpha} \vec{v}_{\alpha}}{v_{\alpha}^3} \quad (41)$$

and the frictional force vector,

$$\frac{\vec{F}_{\alpha\beta}}{A_{\alpha\beta}} = -2 \vec{v}_{\alpha} \frac{1}{m_{\beta} v_{\alpha}^3}. \quad (42)$$

Expressing now the velocities of the test particles in terms of their momenta in Eqs.(41) and (42) yields for the collisional flux $\vec{S}_{\alpha\beta}$,

$$\begin{aligned} \tilde{S}_{\alpha\beta} = & -m_\alpha A_{\alpha\beta} \frac{\gamma_\alpha}{p_\alpha^3} \left\{ \left[\left(1 - \gamma_\alpha^2 \frac{\langle m_\alpha^2 v_\beta^2 \rangle}{p_\alpha^2} \right) p_\alpha^2 \bar{I} \right. \right. \\ & \left. \left. - \left(1 - \gamma_\alpha^2 \frac{\langle m_\alpha^2 v_\beta^2 \rangle}{p_\alpha^2} \right) \bar{p}_\alpha \bar{p}_\alpha \right] \cdot \frac{\partial f_\alpha}{\partial \bar{p}_\alpha} + 2 \frac{m_\alpha}{m_\beta} \gamma_\alpha \bar{p}_\alpha f_\alpha \right\} \end{aligned} \quad (43)$$

This expression coincides with the one derived in [12] in the limit $\langle v_\beta^2 \rangle \rightarrow 0$.

(b) Moments of the Fokker-Planck Equation

The continuity equation in momentum space, if only collisions are taken into account, is simply

$$\left(\frac{\partial f_\alpha}{\partial t} \right)_c + \sum_\beta \vec{\nabla}_{\bar{p}_\alpha} \cdot \tilde{S}_{\alpha\beta} = 0 \quad (44)$$

The kinetic energy $m_\alpha c^2(\gamma_\alpha - 1)$, momentum (\bar{p}_α) and velocity (\bar{v}_α) moments of Eq.(44) are,

$$\int d^3 p_\alpha \frac{\partial f_\alpha}{\partial t} m_\alpha c^2 (\gamma_\alpha - 1) = - \sum_\beta 2m_\alpha A_{\alpha\beta} \int d^3 p_\alpha \frac{f_\alpha}{p_\alpha} \left(\frac{m_\alpha}{m_\beta} \gamma_\alpha - 2 \frac{\langle v_\beta^2 \rangle}{c^2} \right) \quad (45)$$

$$\int d^3 p_\alpha \frac{\partial f_\alpha}{\partial t} \bar{p}_\alpha = - \sum_\beta 2m_\alpha A_{\alpha\beta} \int d^3 p_\alpha f_\alpha \frac{\gamma_\alpha}{p_\alpha^3} \left(\frac{m_\alpha}{m_\beta} \gamma_\alpha + 1 \right) \bar{p}_\alpha \quad (46)$$

and

$$\int d^3 p_\alpha \frac{\partial f_\alpha}{\partial t} \bar{v}_\alpha = - \sum_\beta 2A_{\alpha\beta} \int d^3 p_\alpha \frac{f_\alpha}{p_\alpha^3} \left(1 + \frac{m_\alpha}{m_\beta \gamma_\alpha} - \frac{\langle v_\beta^2 \rangle}{c^2} \right) \quad (47)$$

where one can drop $\langle v_\beta^2 \rangle / c^2$ since the field particles have already been taken as non-relativistic. In our case the field species consists of thermal electrons and thermal ions of densities n_e and n_i respectively. To the extent that the energetic species (the relativistically treated test electrons, e') is a minority species, i.e. $n_{e'} \ll n_e$, the quasineutrality condition is

$$n_e \simeq Z_i n_i \quad (48)$$

where Z_i is the ionic charge number. Therefore in our case Eqs. (45), (46) and (47) take the relatively simpler form,

$$\frac{d^c}{dt} \langle \gamma \rangle = -\nu_c \left\langle \frac{\gamma}{(\gamma^2 - 1)^{1/2}} \right\rangle \quad (49)$$

$$\frac{d^c}{dt} \langle \gamma \tilde{\beta} \rangle = -\nu_c \left\langle \frac{aZ_i + 1 + \gamma}{(\gamma^2 - 1)^{3/2}} \gamma^2 \tilde{\beta} \right\rangle \quad (50)$$

and

$$\frac{d^c}{dt} \langle \tilde{\beta} \rangle = -\nu_c \left\langle \frac{aZ_i + 1 + 1/\gamma}{(\gamma^2 - 1)^{3/2}} \gamma \tilde{\beta} \right\rangle \quad (51)$$

where the angular brackets denote integration over the energetic electron distribution function, and the operator $\frac{d^c}{dt}$ is defined as $\frac{d^c}{dt} \langle \dots \rangle = \int \dots \left(\frac{\partial f}{\partial t} \right)_c d^3p$. The energetic electron subscript has been suppressed. Furthermore, the quantities ν_c and a are defined as follows,

$$\nu_c = \frac{4\pi e^4 n_e \ln \Lambda_{e'e}}{m_e^2 c^3}, \quad a = \frac{\ln \Lambda_{e'i}}{\ln \Lambda_{e'e}} \quad (52)$$

For moderately relativistic electrons and $Z \simeq 1$ the parameter a can be approximated by unity. In all other cases the Coulomb logarithms are given by, [12]

$$\ln \Lambda_{e'e} = \ln \left[\frac{\lambda_{De} m_e c^2 \langle \gamma \rangle \langle \beta \rangle^2}{2(\langle \gamma \rangle + 1)^{1/2} e^2} \right], \quad \ln \Lambda_{e'i} = \ln \left(\frac{\lambda_{De} m_e c^2 \langle \gamma \rangle \langle \beta \rangle^2 \sqrt{2}}{2Z_i e^2} \right) \quad (53)$$

where λ_{De} is the electron-Debye length.

(c) Fokker-Planck and Quasilinear Evolution, and Steady State

In the presence of an externally imposed driving mechanism (RF waves in particular) the evolution equations Eqs.(49) to (51) take the form,

$$\frac{d}{dt} \langle \gamma \rangle = -\nu_c \left\langle \frac{\gamma}{(\gamma^2 - 1)^{1/2}} \right\rangle + P_d \quad (54)$$

$$\frac{d}{dt} \langle \gamma \vec{\beta} \rangle = -\nu_c \left\langle \frac{Z_i + 1 + \gamma}{(\gamma^2 - 1)^{3/2}} \gamma^2 \vec{\beta} \right\rangle + F_d \quad (55)$$

and

$$\frac{d}{dt} \langle \vec{\beta} \rangle = -\nu_c \left\langle \frac{Z_i + 1 + 1/\gamma}{(\gamma^2 - 1)^{3/2}} \gamma \vec{\beta} \right\rangle + A_d \quad (56)$$

where we set $a = 1$. The quantities P_d , F_d and A_d are defined as the input of RF power (P_d) and the macroscopic manifestation of the force and the acceleration (F_d , A_d) associated with the wave-particle interactions. They are normalized to $\nu_c m c^2$, $\nu_c m c$ and $\nu_c c$ respectively.

The simplest evaluation of Eqs. (54)–(56) is for an effective distribution function $f(p_{\parallel}, p_{\perp})$ given by,

$$f(p_{\parallel}, p_{\perp}) = \frac{\delta(p_{\parallel} - \bar{p}_{\parallel}) \delta(p_{\perp} - \bar{p}_{\perp})}{2\pi \bar{p}_{\perp}} \quad (57)$$

where \bar{p}_{\parallel} and \bar{p}_{\perp} correspond to the average, effective values of the parallel and perpendicular momenta. Omitting the overbars for simplicity one now has,

$$\frac{d\gamma}{dt} = -\nu_c \frac{\gamma}{(\gamma^2 - 1)^{1/2}} + P_0 \quad (58)$$

$$\frac{d}{dt} (\gamma \beta_{\parallel}) = -\nu_c \frac{Z_i + 1 + \gamma}{(\gamma^2 - 1)^{3/2}} \gamma^2 \beta_{\parallel} + F_0 \quad (59)$$

$$\frac{d\beta_{\parallel}}{dt} = -\nu_c \frac{Z_i + 1 + 1/\gamma}{(\gamma^2 - 1)^{3/2}} \gamma \beta_{\parallel} + A_0 \quad (60)$$

where the P_0 , F_0 and A_0 refer to the RF quantities P_d , F_d and A_d , respectively, for the distribution function of Eq. (57). Consistency of these three equations, namely Eq.(59) being derivable from Eqs.(58) and (60), implies that,

$$A_0 = \frac{F_0}{\gamma} - \beta_{\parallel} \frac{P_0}{\gamma} \quad (61)$$

Solution of Eqs. (58)–(60) in the steady state, in the sense of $\frac{d}{dt} \langle \gamma \rangle = \frac{d}{dt} \langle \gamma \beta_{\parallel} \rangle = 0$, finally yields,

$$P_0 = \frac{\gamma}{(\gamma^2 - 1)^{1/2}} \quad (62)$$

$$\beta_{\parallel} = \left[\frac{\gamma^2 - 1}{\gamma(Z + \gamma + 1)} \right]^{1/2} \quad (63)$$

and

$$F_0 = \frac{P_0}{\beta_{\parallel}} \quad (64)$$

The first equation Eq. (62) provides the relationship between the RF power input and the average energy ϵ (in normalized units $\epsilon = \gamma - 1$) of the energetic electrons. Equation (63), on the other hand, gives the current these electrons are carrying. Finally Eq. (64) is the macroscopic manifestation of the relationship between power dissipated (normalized to $\nu_c mc^2$) and force dissipated (normalized to $\nu_c mc$) in the case of resonant diffusion induced by a unidirectional RF wave [14].

In Figure 4 β_{\parallel} and the normalized figure of merit, namely the ratio β_{\parallel}/P_0 , are plotted as functions of ϵ and for $Z_i = 1$; for a given density n_e , at an energy ϵ the current density is $|J_{\parallel}| = en_e c \beta_{\parallel}$. For $\epsilon \gg 1$, both β_{\parallel} and the ratio β_{\parallel}/P_0 approach unity. We note that

$$\frac{\beta_{\parallel}}{P_0} = \frac{(\epsilon + 1)^2 - 1}{(\epsilon + 1)^{3/2}(\epsilon + 2 + Z_i)^{1/2}} \equiv f(\epsilon, Z_i) \quad (65)$$

gives

$$\frac{J}{p_D} = \frac{e}{mc\nu_c} f(\epsilon, Z_i) \quad (66)$$

Thus the figure of merit is found to be

$$\left(\frac{I}{P_D} \right)_{\frac{\text{Amp}}{\text{Watt}}} = \frac{31.2 f(\epsilon, Z_i)}{\ln \Lambda R_m n_{20}} \quad (67)$$

where R_m is the major radius of the tokamak in meters and n_{20} is the plasma density in units of $10^{20}/m^3$. In the nonrelativistic limit, $\epsilon \ll 1$, $f \sim \epsilon$ and the figure of merit increases for current carried by more energetic electrons. In the ultrarelativistic limit, $\epsilon \gg 1$, $f \rightarrow 1$ and Eq.(67) gives an upper bound on the figure of merit. Recent experiments on PLT and Alcator C can be considered to be effectively in the range $\epsilon \approx 0.1 - 0.2$. Considerable improvement in the figure of merit is therefore possible by RF current drive with more energetic electrons. This should be possible with the use of the fast wave in the lower-hybrid range of frequencies. The limit will most likely be dictated by how well energetic electrons can be confined in the plasma.

Finally, taking into account Eq. (63) and the identity $\gamma^2 = 1 + q_{\parallel}^2 + q_{\perp}^2$, with q_{\parallel} and q_{\perp} being the normalized parallel and perpendicular momentum respectively (note that $q_{\parallel} = \gamma\beta_{\parallel}$), yields for $Z_i = 1$,

$$q_{\parallel} = \frac{q_{\perp}}{2} \left[\frac{q_{\perp}^2 + (q_{\perp}^4 + 16q_{\perp}^2 + 16)^{1/2}}{2} \right]^{1/2}. \quad (68)$$

In Fig. (5) q_{\perp}^2 , which is a measure of the perpendicular, randomly oriented momentum of the fast electrons in the steady state operation, is plotted as a function of the normalized parallel momentum q_{\parallel} . We thus note that in the steady-state larger parallel momenta must have associated larger, random perpendicular momenta. This is in concert with the enhanced perpendicular temperature effect described by the nonrelativistic numerical and theoretical results of sections II and III. We are currently in the process of generating numerical solutions of the relativistic Fokker-Planck equation with quasilinear diffusion as formulated in this section.

V. ACKNOWLEDGEMENT

The authors would like to thank J. Freidberg, A. Ram and M. Shoucri for helpful discussions and criticisms. In addition, D. H. and V. K. thank C. Karney likewise.

This work was supported by DOE Contract No. DE-AC02-78ET-51013.

APPENDIX 1

The important detail of the solution process resides in the numerical implementation of the algorithm taking the initial f_1 to the time asymptotic state. The usual approach is to simply finite difference the terms in Eq. (1), select a time step Δt small enough for stability, and time integrate the initial distribution to the final configuration. This is a straightforward procedure although it frequently becomes quite expensive computationally if a fully explicit time advance is used. We have achieved a quite significant reduction in the computer time required to get to the asymptotic state by employing two additional techniques.

Firstly, the maximum Δt that can be used in a stable integration scheme – which is proportional to the minimum grid resolution length squared for explicit schemes – is considerably increased by using a alternating-direction-implicit (ADI) procedure for the time advance [15]. Secondly, it is reasonable to assume that during the integration from the initial to the asymptotic state there will be periods for which is desirable (indeed necessary for stability) to take small Δt s. Similarly there are also periods during which not much change in f is occurring and much CPU time can be saved by increasing the Δt . What we have implemented for this work is an adaptive Δt selection procedure which, for reason that will become apparent, we call Aggressive ADI (AADI).

In the procedure we now outline, the guiding principle is that we want to achieve the asymptotic state as fast as possible. This goal is achieved by using as few time steps as possible consistent with stability of the solution. We are not particularly concerned with the details of the time evolution providing we can convince ourselves that the final state is independent of its evolution. We define the residue ϵ as

$$\epsilon \equiv \left. \frac{\partial f}{\partial \tau} \right|_{max}$$

where the subscript *max* refers to the maximum absolute value across the entire u, μ mesh. The concept is simple; we increase the Δt on successive time steps until the ϵ increases. As long as ϵ decreases, the solution is considered acceptable up to that "time" level and ϵ is saved for future comparison. For an operator which

is dominated by the diffusive terms (from velocity and pitch angle scattering), an increasing ϵ indicates the onset of instability. Δt is gradually increased until ϵ no longer decreases. We follow this last time step, which is on the verge of instability, by a smaller Δt which is intended to allow the solution to stabilize itself. If a reevaluation of ϵ confirms that the solution is again stable (ϵ is again decreasing), the new solution is accepted, and another time step is taken with the same time step size that is near the stability limit *at this time in the integration*. If the small step does not stabilize the solution, a second small step is taken in a final attempt to stabilize the solution. Should it succeed, we are making optimal progress toward the asymptotic limit; should it fail, the last big step and these two small steps are discarded, the solution is restored at the last acceptable configuration, and Δt is reduced substantially before an attempt is made to continue the solution.

This procedure provides for aggressive increases in Δt to the stability limit during periods of inactivity in the time dependence of f_1 . Should the activity increase, a rapid retrenchment is triggered which is very protective of the solution. If a situation is encountered in which the only solution requires an increase in ϵ , this algorithm will fail. The signature of such a mode is that no further time steps are "acceptable" and Δt is reduced to a very small number. This mode is never observed in the present application to Eq. 1.

There are obviously several adjustable parameters which must be selected to optimize this procedure; the most important are the ratio of the stabilizing step size to the large step size and the factor which multiplies Δt when the solution cannot be stabilized, typically .5 and .1 respectively, for this particular operator on our 80 by 60 mesh. Typically 500 time steps are required to obtain a solution f_1 which no longer changes in any significant way. These runs require no more than 60 CPU seconds on a CRAY 1 for D_0 less than one.

REFERENCES

1. M. Porkalab, et al., *Proc. 9th Int. Conf. on Plasma Phys. and Contr. Nucl. Fusion Res.* (Baltimore, U.S.A., Sept. 1982), I.A.E.A., Vienna 1983, Vol. I, pp. 227-236.
B. Lloyd et al. in Proceedings of this meeting.
2. W. Hooke et al., *Proc. 9th Int. Conf. on Plasma Phys. and Contr. Nucl. Fusion Res.* (Baltimore, U.S.A., Sept. 1982), I.A.E.A., Vienna 1983, Vol. I, pp. 239-245.
S. Bernabei, et al., *Phys. Rev. Lett.* 49, 1255 (1982).
R. Motley, et al., in Proceedings of this meeting.
3. S. Von Goeler et al., *Bull. Amer. Phys. Soc.* 27, 1069 (1982).
4. M. Porkolab et al., *Proc. 5th Top. Conf. on RF Plasma Heating*, Madison, Wisc., 1983.
S. Texter, M.I.T.-P.F.C. (private communication, 1983).
5. R. Klima and V. L. Sizonenko *Plasma Physics*, 17, 463 (1975).
6. N. J. Fisch, *Phys. Rev. Lett.* 41, 873 (1978).
7. C.F.F. Karney and N.J. Fisch, *Phys. Fluids* 22, 1817 (1979).
8. A. V. Gurevich, *ZhETF* 39, 1296 (1960); *Sov. Phys. - JETP* 12, 904 (1960).
A. N. Lebedev, *ZhETF* 48, 1939 (1965); *Sov. Phys. - JETP* 21, 931 (1965).
9. N. J. Fisch, *Phys. Rev.* A24, 3245 (1981).
10. K. Hizanidis, K. Molvig, and K. Swartz, MIT Plasma Fusion Center Report PFC/JA-81-21 (1981); to appear in the *Journal of Plasma Physics*.
11. V. P. Silin, *Soviet Physics, JETP* 13, 1244 (1961).
12. I. B. Bernstein, D.C. Baxter, Science Applications Inc.- Laboratory for Applied Plasma Studies, UC-20,G, Report No. LAPS-68 SAI-023-80-352-LJ, May 1980.
13. D. Mosher, *Phys. Fluids* 18, 846 (1975).
14. A. Bers in *Plasma Physics - Les Houches 1972*, Eds. C. DeWitt and J. Peyrand, Gordon and Brach Science Publishers, 1975, p. 133.
15. R.D. Richtmyer and K.W. Morton, *Difference Methods for Initial-Value Problems*, Wiley (1967).

FIGURE CAPTIONS

Figure 1 The computational region is an annular region. In spherical coordinates the velocity magnitude u ranges from u_{min} to u_{max} ; the polar angle θ is expressed by $\mu \equiv \cos \theta$ and μ varies between -1 and 1. The solution is found on a uniform orthogonal mesh in the u, μ space within this region.

Figure 2 (a) Logarithmic contours of the distribution function f for RF spectrum parameters: $D_0 = 1.0$, $v_0 = 4.0$, $\Delta v = 1.0$, and $p = 4$. The contour values begin with 1×10^{-8} on the outermost contour and increase monotonically to 0.7 on the innermost contour. Contour values of 1, 4, and 7 are plotted for each decade. (Eight decades are shown.) Salient features include the stretching of f in the $v_{||}$ direction in the region containing appreciable $D(v_{||})$ and an enhanced temperature in both T_{\perp} and $T_{||}$ due to this stretching.

(b) The perpendicular temperature $T_{\perp}(v_{||})$ for the distribution function shown in (a). The temperature of the inner core distribution is unity. T_{\perp} increases rapidly to nearly 4 as $v_{||}$ moves through the rf spectrum. For $v_{||} > 6$ the applied rf rapidly diminishes but the perpendicular temperature continues to rise. In this particular case, the mesh only extended to $u_{max} = 12$. Consequently, as $v_{||}$ approaches u_{max} , the information available (nearby grid points) to perform an accurate integration over v_{\perp} rapidly shrinks to zero; and the precise behavior of T_{\perp} is suspect for $v_{||} \geq 10$.

Figure 3 (a) In this plot are displayed logarithmic contours of f similar to those in Fig. 2a with different parameters in $D(v_{||})$. Compared to Fig. 2, this spectrum, while still having the same amplitude, $D_0 = 1.0$, has been broadened $\Delta v = 2.0$, has been made less abrupt, $p = 2$, and has been centered at a larger velocity $v_0 = 6.0$.

(b) The perpendicular temperature $T_{\perp}(v_{||})$ for the distribution function shown in a). Since u_{max} is much larger in this case than in Fig. 2, much more confidence can be given to the behavior of T_{\perp} for $v_{||}$ above the rf spectrum. As explained in Sec. III, the T_{\perp} within the spectrum is larger than in Fig. 2 because v_1 is larger. In the external region, T_{\perp} continues to rise as in Fig. 2. However in this case, enough grid resolution is available to indicate that T_{\perp}

does approach the asymptotic value of 1 for very large v_{\parallel} .

Figure 4 The normalized parallel current β_{\parallel} and the normalized figure of merit β_{\parallel}/P_0 (the dashed line is the nonrelativistic limit) are plotted as functions of the normalized kinetic energy $\epsilon = \gamma - 1$ for $Z_i = 1$.

Figure 5 q_{\perp}^2 is plotted as a function of the normalized parallel momentum $q_{\parallel} = \gamma\beta_{\parallel}$ for $Z_i = 1$.

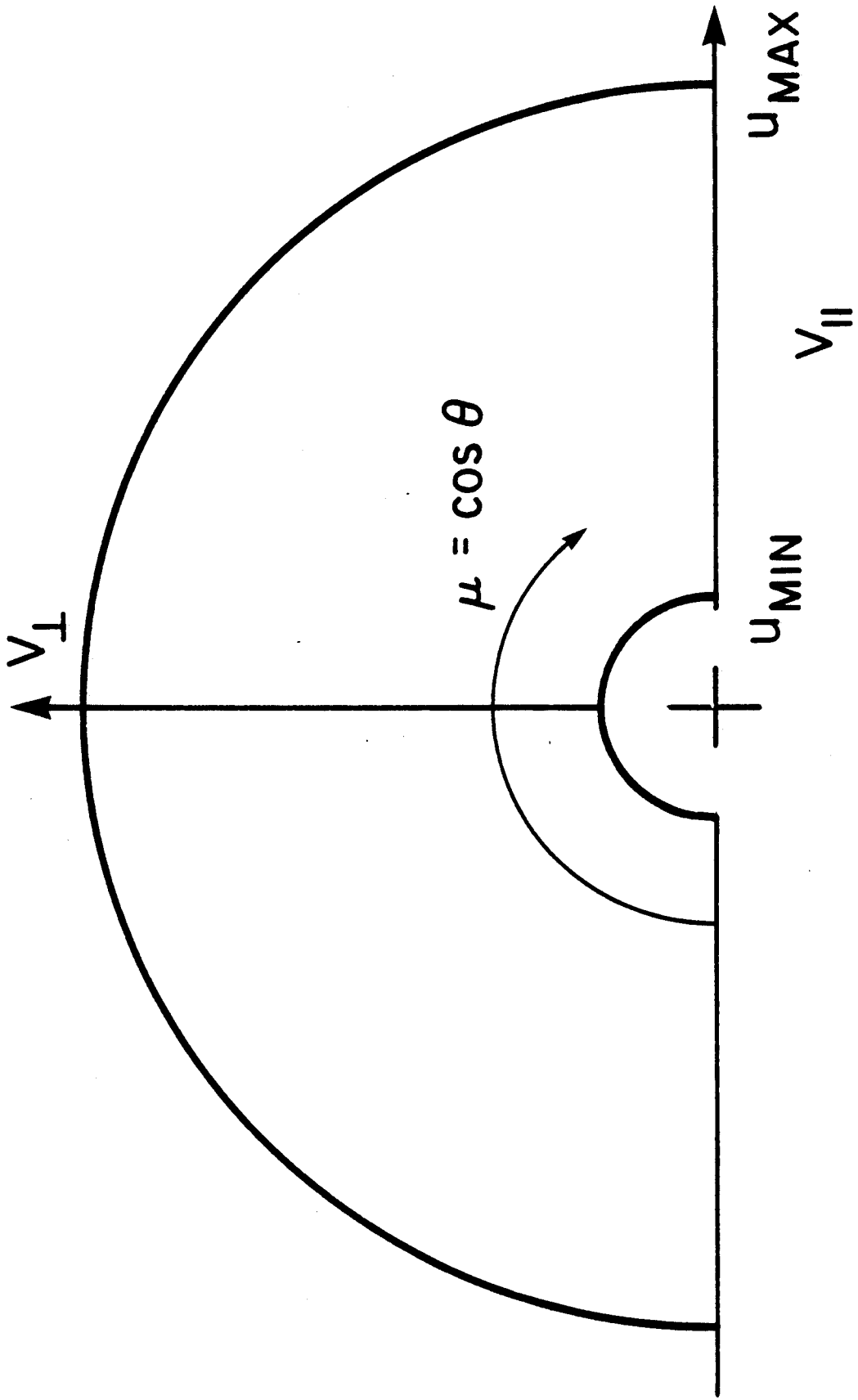


FIGURE 1

LOGARITHMIC CONTOURS OF f

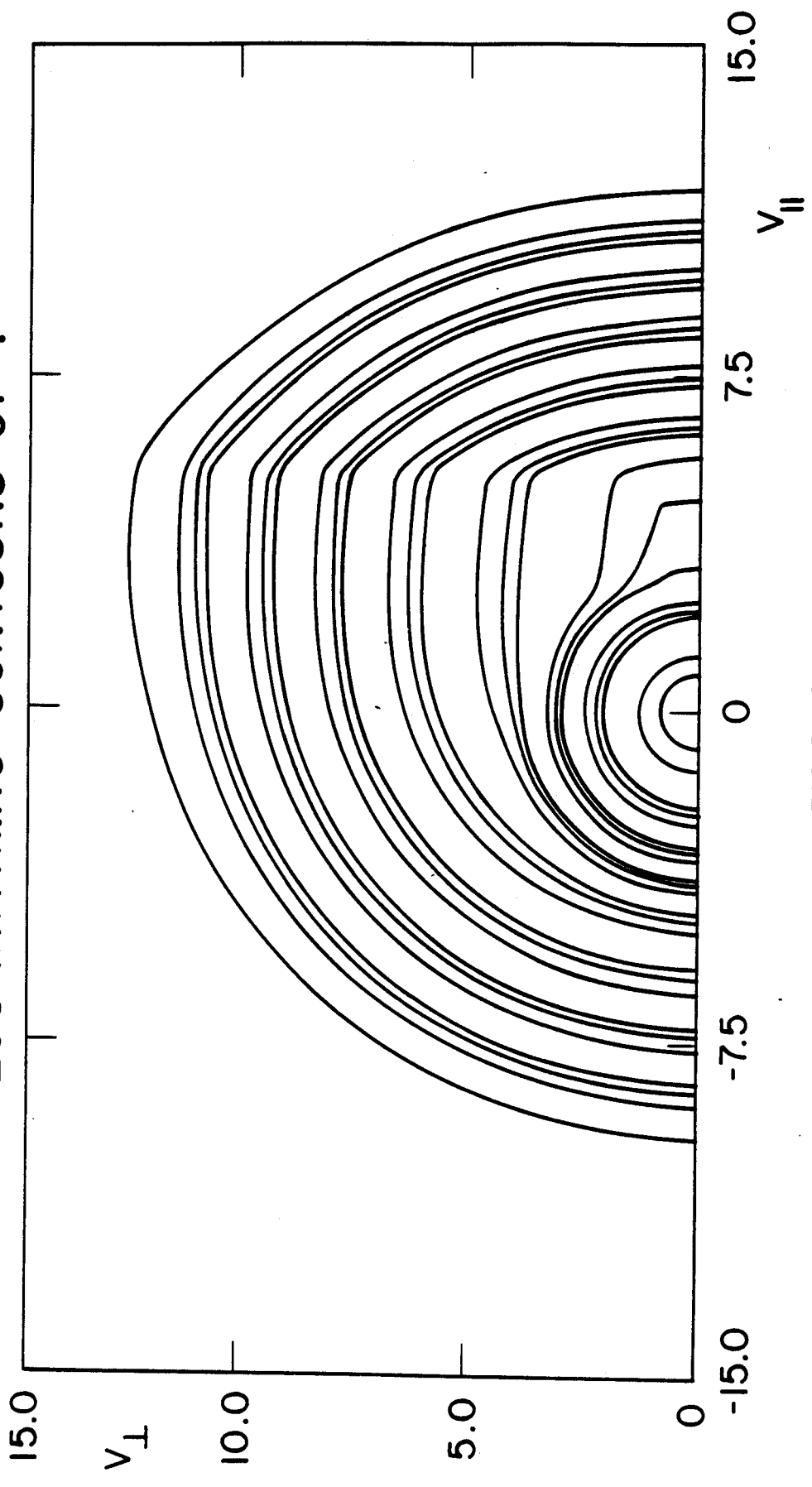


FIGURE 2 (A)

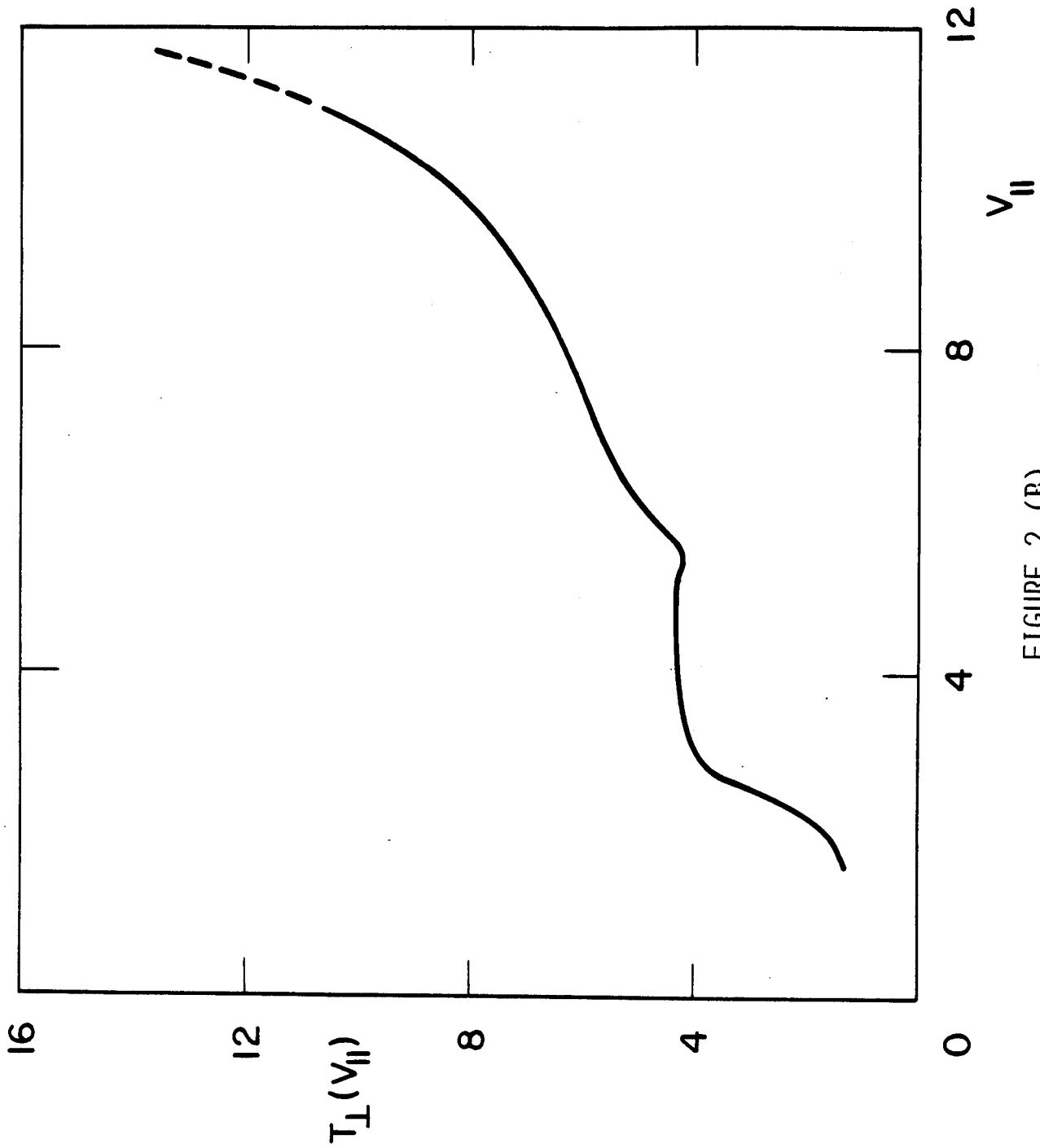


FIGURE 2 (B)

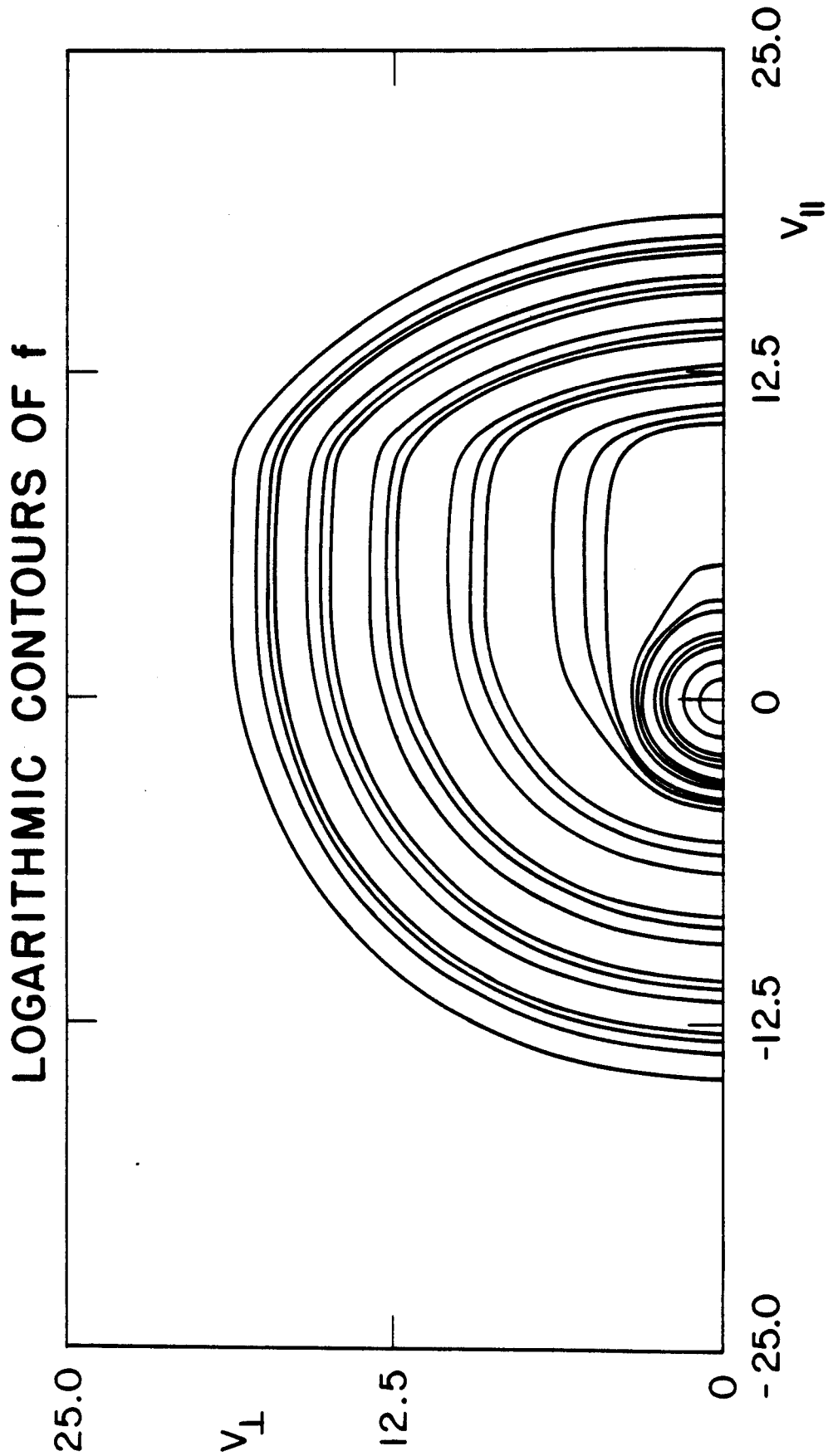


FIGURE 3 (A)

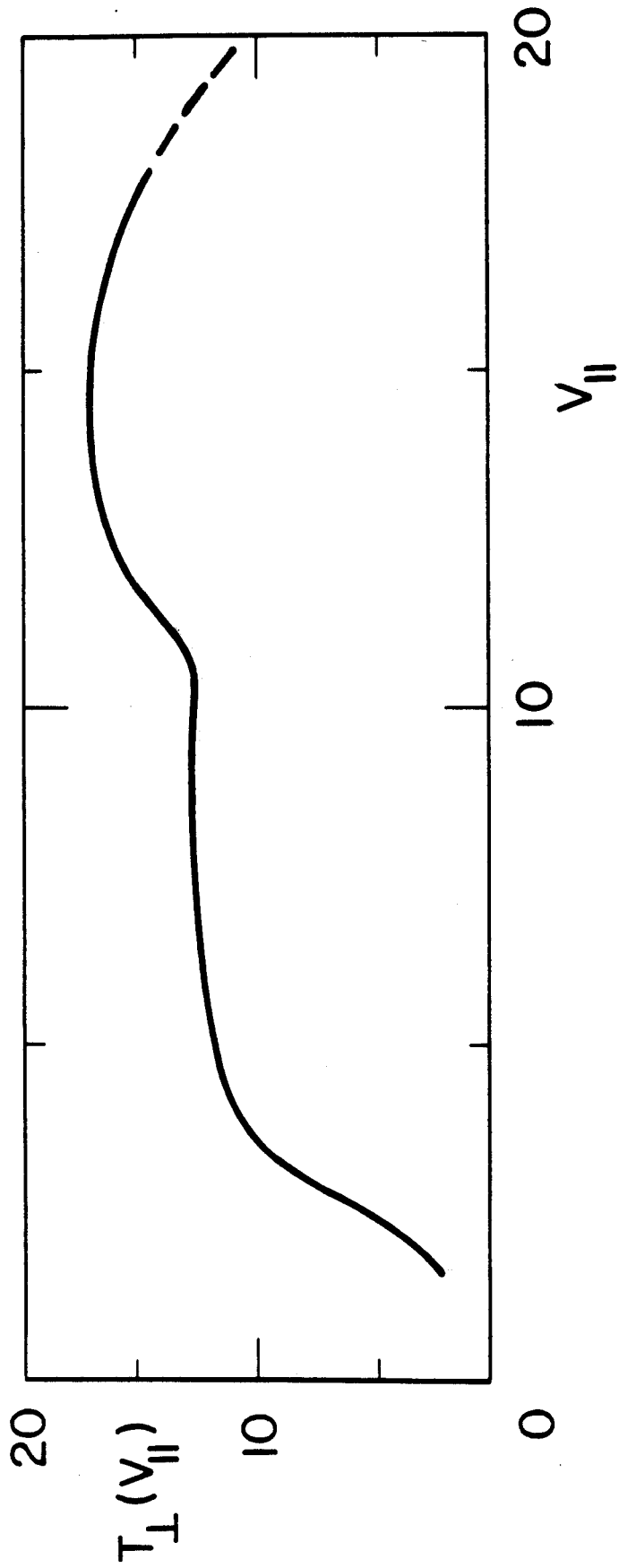


FIGURE 3 (B)

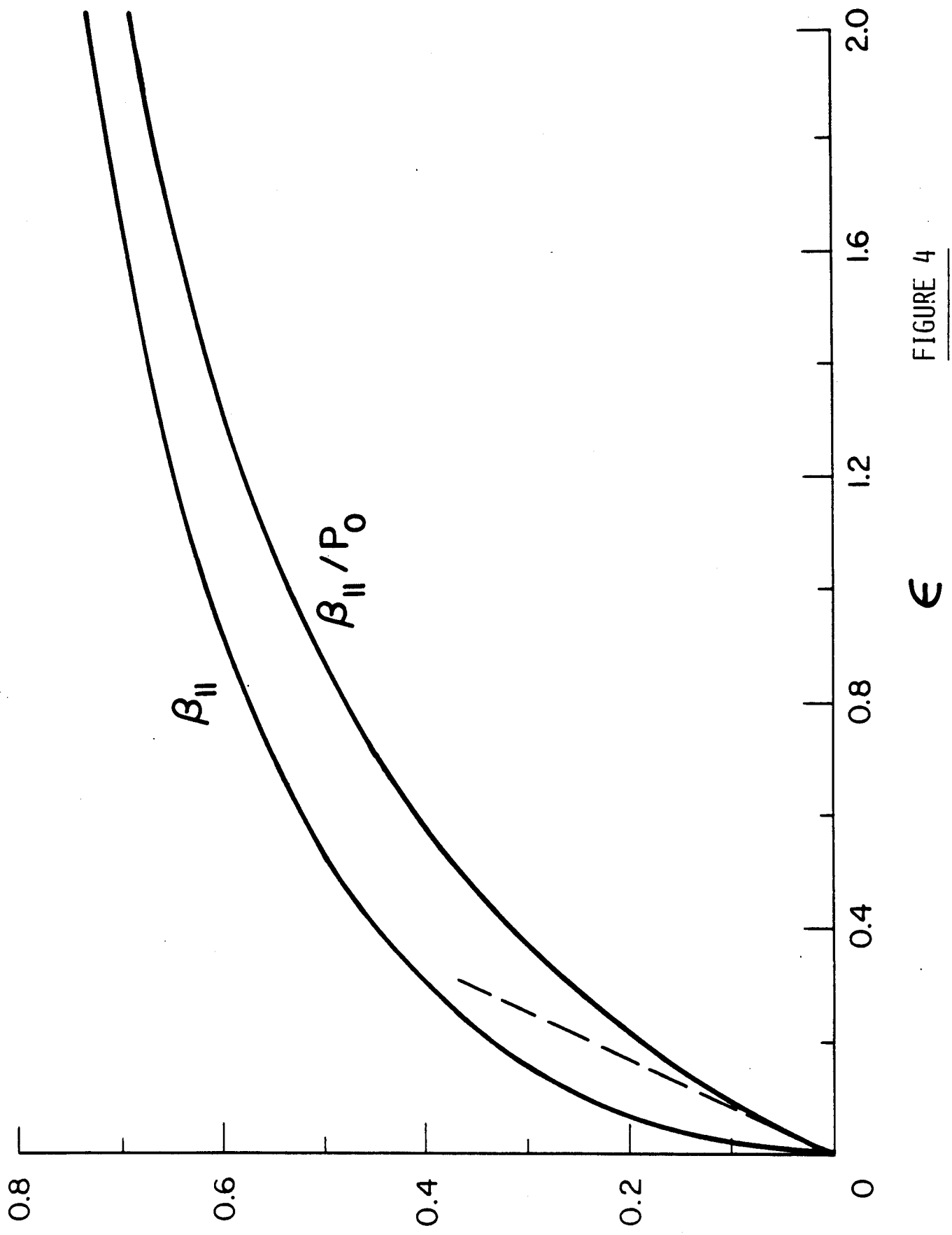


FIGURE 4

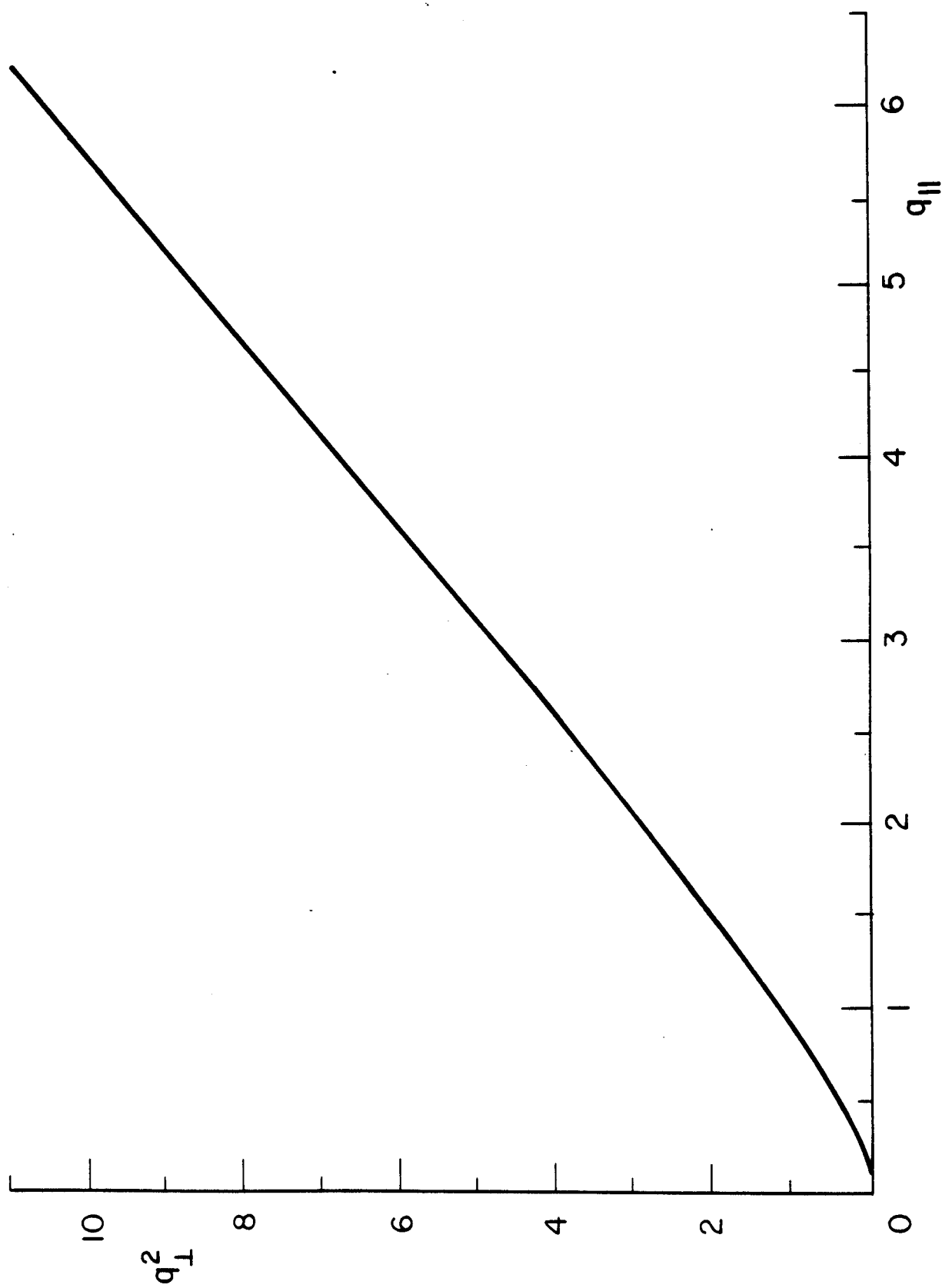


FIGURE 5